SHORT WAVE INSTABILITIES OF COUNTER-ROTATING BATCHELOR VORTEX PAIRS

Kris RYAN, Gregory J. SHEARD and Mark C. THOMPSON

Fluids Laboratory for Aeronautical and Industrial

Research (FLAIR), Department of Mechanical Engineering, Monash University,

Melbourne, Victoria 3800, Australia

ABSTRACT

Recently, investigations have considered the cooperative elliptic instability which forms by the mutual co-existence of a counter-rotating Batchelor-type vortex pair. Such vortex pairs are observed in the wake of an aircraft and pose a significant danger to trailing aircraft. An aircraft flying through the wake of a lead aircraft can exhibit significant loss of lift and control forces; several accidents and near-misses have been recorded. Our investigation has identified that short-wave Kelvin-type instabilities may prematurely destroy the vortex pair. By inducing short-wave instabilities there is the potential to significantly improve safety in the aviation industry. The work has relied heavily on CFD to validate analytical estimates and provide data for future experimental investigations.

NOMENCLATURE

a characteristic vortex core radius
a_0 initial characteristic vortex core radius
b   vortex separation distance
k axial wavenumber
q swirl number
r radial dimension
t time
t^* time coefficient
t_c characteristic growth time
u_θ azimuthal velocity component
z axial dimension
Re Reynolds number
U self advection velocity
W axial velocity component
W_0 axial velocity coefficient

λ axial wave length
$\boldsymbol{q}$ azimuthal dimension
Γ circulation
$\boldsymbol{r}$ density
σ instability growth rate
$\boldsymbol{n}$ kinematic viscosity
σ^* normalized instability growth rate
ε_0 external strain rate
ω_0 vorticity

INTRODUCTION

Trailing vortices form in the wake of aircraft as a result of the lifting process. High pressure air from the lower surface of the wings migrates to the low pressure air located above the upper surface of the wings, the practical result of which is a localized rotational flow at the wing tips, known as trailing vortices. Trailing vortices persist for a considerable length of time and pose a significant hazard to the flight characteristics of an aircraft following the lead aircraft. The strength and time to dissipation of the trailing vortices are strongly dependent on the weight, size and lift coefficient of the aircraft. This last point presents serious issues especially at take-off and landing. Far downstream of the aircraft, the two vortices form a counter-rotating vortex pair, each of which have an additional velocity component in line with the axis of the vortex. This velocity component occurs purely due to the forward motion of the aircraft through the air.

Flow Field Description

In this study two counter-rotating Batchelor vortices are placed a distance b apart. Each vortex has a characteristic radius a. Each vortex imposes a weak irrotational strain field on the other which is referred to as the external strain field, $\boldsymbol{e}_0$ (for example see Le Dizès and Laporte (2002)). This paper is restricted to the study of counter-rotating vortices in order to avoid two-dimensional merging phenomenon observed for co-rotating vortices (as observed by Le Dizès and Verga (2002) among others).
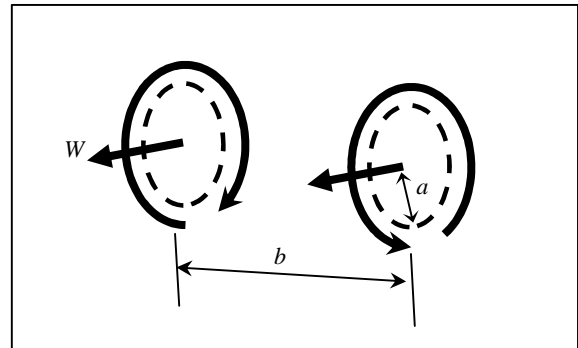
Figure 1: Schematic diagram of geometry.

Each vortex investigated has the generic Gaussian profile, expressed in cylindrical co-ordinates ($r, \boldsymbol{q}, z$) centred at the vortex centre:

$$\boldsymbol{w}_0 = \frac{\Gamma}{\boldsymbol{p}\, a_0^2}\, e^{\frac{-r^2}{a_0^2}},$$

$$W = \frac{W_0\Gamma}{\boldsymbol{p}\, a_0^2}\, e^{\frac{-r^2}{a_0^2}}. \qquad (1)$$

Here a_0 is the characteristic core radius of the vortex at time $t = 0$, and W_0 is the axial velocity coefficient, defined as:

$$W_0 = \frac{\hat{W}}{\hat{u}_{\boldsymbol{q}}} = \frac{1}{q}, \qquad (2)$$

where $\hat{u}_{\boldsymbol{q}}$ is the maximum azimuthal velocity component, $\hat{W}$ is the maximum axial velocity component and q is the swirl number. Such a vortex profile was first proposed by Batchelor (1964) as representative of the profile of a trailing line vortex in the wake of an aircraft. For the case where $W_0 = 0$, the vortex profile (equation 1) reverts to a Lamb-Oseen type, which has previously been investigated Sipp and Jacquin (2003). In isolation, the Batchelor vortex represents a stationary solution to the Euler equations, and a complete solution to the Navier-Stokes equations.

It has been shown that a vortex with a Gaussian profile is a known global attractor of any two-dimensional axisymmetric vortex (see for example Batchelor (1964); all axisymmetric two-dimensional vortices relax by viscous diffusion to the Lamb-Oseen vortex profile. It is anticipated *a priori* that the Batchelor vortex will similarly represent a global attractor for flows with an axial velocity component. The Gaussian profile has the advantage over other possible profiles, in that it is unaffected by viscous diffusion. Viscosity only acts to modify the radius of the vortex, which evolves linearly in time (Batchelor (1964)) and has been shown to evolve as:

$$a(t) = \sqrt{a_0^2 + 4\boldsymbol{n}\, t}, \qquad (3)$$

where $\boldsymbol{n}$ is the viscosity of the fluid. Assuming a sufficiently large Reynolds number, the vortex core size may be considered constant over the linear growth period of an instability.

Several studies have investigated the growth of instabilities for the case of a Batchelor type vortex in isolation. Ash and Khorrami (1995), in an investigation limited to inviscid flows, found that an isolated Batchelor-type vortex was unstable to Kelvin type instabilities for a minimum swirl number (q) of approximately 1.5 (corresponding to a maximum axial velocity coefficient $W_0 \approx 0.677$. More recently, Fabre *et al.* (2004) studied the effect of viscous forces which are known to induce both axisymmetric and symmetric instability modes, their investigation concluding that these modes had a long wavelength, and growth rates orders of magnitude smaller than those found by Ash and Khorrami (1995). On the basis of these investigations, the axial velocity coefficient has been restricted to the range $W_0 = [0,0.6]$, such that the destabilizing effect of one vortex on the other may be studied in isolation.

Prior Investigations

A large wavelength instability known as the Crow instability has previously been observed in the trailing vortex system which assists with the dissipation of the trailing vortices (Crow (1970)). The Crow instability describes the growth in amplitude of a sinuous oscillation of each of the vortex cores due to the presence of the other vortex in the pair. As the instability mode grows over time, the two vortex lines merge to form vortex rings and rapidly dissipate to form small-scale turbulent structures thereafter. Crow (1970) analytically determined the wavelength and growth rate of this form of instability. However his investigation was limited to large wavelength instabilities, as his analytical model approximated each vortex as an infinitesimally small vortex line. While the Crow instability has been identified as the dominant instability occurring in the trailing wake of an aircraft, the growth rate is relatively small. Crow (1970) found a normalized growth rate $\sigma^* \approx 0.8$, where,

$$\boldsymbol{s}^* = \frac{\boldsymbol{s}}{\Gamma/2\boldsymbol{p}b^2}. \qquad (4)$$

Here, σ is the growth rate of the instability, where all velocity components increase over time following the function:

$$(u, v, w) = (u_0, v_0, w_0)e^{\boldsymbol{s}t}. \qquad (5)$$

Due to the low growth rate, the wake structures from large aircraft remain coherent for an extensive period of time forcing following aircraft to wait considerable lengths of time at airports for the trailing vortex system to dissipate.
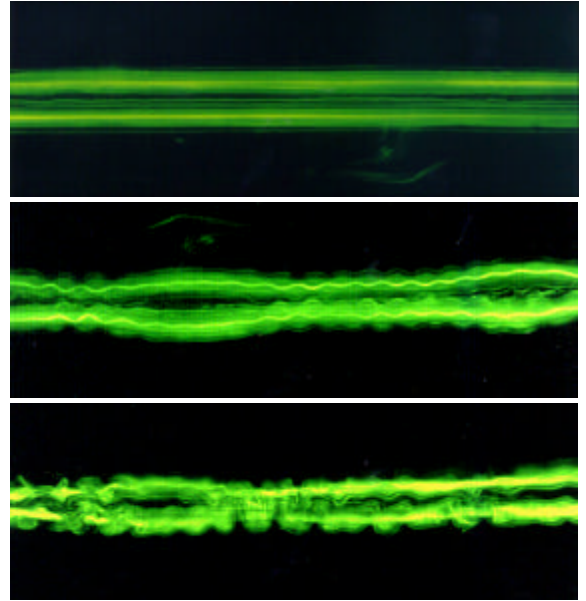
Figure 2: Die visualization of a vortex pair, showing growth of a long-wave Crow instability coupled with a short wave Kelvin mode instability (mode -1,1). From Leweke and Williamson (1998).

More recently, research into elliptic, short-wave instabilities of vortex pairs has found renewed interest as a phenomenon which could be used to accelerate the dispersion of trailing vortices (Leweke and Williamson (1998), Meunier and Leweke (2005), and Lacaze *et al.* (2006)) Elliptic, short-wave instabilities occur due to the

strain field produced within one vortex core due to the presence of the second vortex. Several investigations have confirmed that Kelvin mode pairs, neutrally stable for an isolated vortex, may grow to form short wave instabilities due to the presence of a second vortex. Recently, both experimental and numerical investigations have considered the instability mechanisms for counter-rotating (Leweke and Williamson (1998) and co-rotating (Meunier and Leweke (2005)) vortex pairs, for vortices with no axial velocity component. For both cases, a short-wave, sinusoidal oscillation was found to grow in each vortex, corresponding to a resonance of the (-1,1) Kelvin modes in each vortex (see figure 2). Leweke and Williamson (1998) observed an elliptic Kelvin mode superimposed on the large wavelength, Crow instability. They observed that the addition of the short wavelength instability resulted in a 20% increase in the normalized growth rate σ^* at a Reynolds number, $Re = 2800$, where the Reynolds number is defined based on the circulation within each vortex as $Re = \frac{G}{n}$. They predicted the normalized growth rate should increase with increased Reynolds numbers. Meunier and Leweke (2005) found a similar result when considering a co-rotating vortex pair. Neither study observed a short-wave elliptic instability in the presence of even a small axial velocity component; hence their findings were not directly applicable to the aircraft wake problem.

The short-wave instability mode identified by Leweke and Williamson (1998) and Meunier and Leweke (2005) is only one of several Kelvin type instabilities which may propagate within a vortex. Prior to these investigations, several studies have determined the structure of Kelvin modes for a variety of flow fields. For the case of a vortex with uniform vorticity whose radial dimension is confined to a finite value (a Rankine vortex), the Kelvin modes form a basis for perturbations confined within the vortex core (Arendt et al. (1997)).
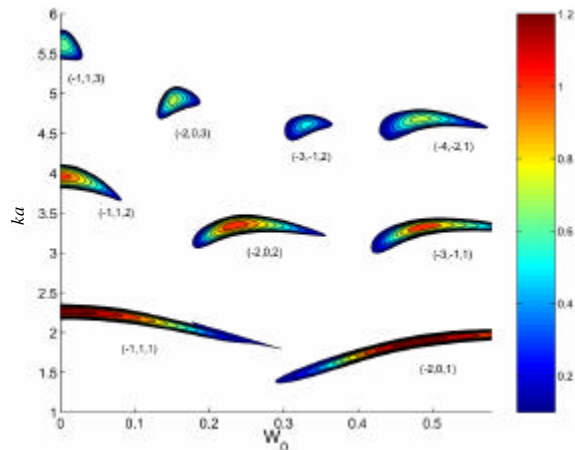
Figure 3: Instability area of the principal coupling modes in a plane (W_0, ka). Colours correspond to the intensity of the growth rate (from blue to red: from minimum to maximum) for $Re = 20\,000$ and $\varepsilon_0 = 0.01$. From Lacaze et al. (2006).

More recent investigations have considered the case of non-uniform vortices. Sipp and Jacquin (2003) and Fabre et al. (2004) have investigated the structure of Kelvin modes for the case of a vortex of Gaussian cross section in

the absence of an axial velocity (a Lamb-Oseen vortex). Le Dizes and Lacaze (2005) investigated the effect of adding an axial velocity component on the form of inviscid normal instability modes (Kelvin modes) which may grow in the presence of the Batchelor vortex pair, where each vortex is of the form given by equation 1. Their investigation identified several other Kelvin mode pairs (apart from the mode -1,1 identified in earlier studies) which could occur in the presence of an axial velocity.

A further investigation by Lacaze et al. (2006) analytically determined the normalized growth rates of the short-wave Kelvin mode pairs as a function of W_o and the axial wavenumber k. Analytically, this investigation was initially conducted in an inviscid fluid ($Re \rightarrow \infty$). The effect of a viscous fluid was considered as a damping effect on the growth rates of the instability modes – figure 3 shows the analytically determined growth rates for a range of Kelvin mode pairs for $Re = 20000$. The analytical work was validated by numerical computations which were restricted to solving the linearized Navier-Stokes equations over a range of axial wave numbers. For each axial wave number, the dominant short-wave elliptic instability was identified, and its growth rate was noted. The authors found excellent agreement between the linearized simulations and the analytical investigation.

The goal of this paper is to confirm the findings of Lacaze et al. (2006) by use of three-dimensional direct numerical simulations of two counter-rotating Batchelor-type vortices (i.e. two vortices of Gaussian cross-section, each with a finite axial velocity component).

NUMERICAL TECHNIQUE

A spectral-element method was used for the direct numerical simulations in this investigation. The method employs high-order tensor-product Lagrangian polynomials as shape functions within each element. A Fourier expansion of the velocity and pressure fields was employed in the axial direction.

The three-dimensional method extends the two-dimensional spectral element method by using a global Fourier spectral discretization in the third dimension. This approach has been employed previously for the case of the flow past a circular cylinder by Thompson et al. (1996) among many others. The global spectral approach has the advantage of spectral convergence, however the boundary conditions in the axial direction are restricted to be periodic.

The spatial discretization consists of 16 equi-spaced planes in the span-wise direction, each consisting of an identical spectral-element mesh. The flow variables are transformed into Fourier space in the span-wise direction for each node on the spectral element mesh using a fast Fourier transform. This decouples the problem into a set of 16 Fourier modes which are then solved independently for the linear operators.

The time integration uses a three-step time-splitting method and achieves second-order time accuracy, and is described completely in Karniadakis et al. (1991) The spatial accuracy was determined at run time by specifying

the order of the tensor-product of interpolating polynomials within each macro-element. In all the simulations quoted herein, 700 macro-elements were employed with 8th order polynomial interpolants. A square domain was employed with a domain length and width of 40 vortex diameters.

Throughout this study, the Reynolds number and the normalised vortex separation distance were held fixed at Re=20 000, and $^a/_b = 0.25$ respectively. This corresponded to an external strain rate $e_0 = 0.0625$. When compared to the analytical study of Lacaze et $al.$ (2006), this was a relatively high strain rate. However it was chosen to increase the growth rate of the 3D instabilities (and hence decrease computational expense) while maintaining a sufficiently low strain rate that valid comparisons could be made with the analytical theory of Lacaze et $al.$ (2006).

If the two vortices are localized and sufficiently far apart, each vortex may be represented as a point vortex. This representation provides the inviscid dynamics of the system, and if the viscous effects are negligible to leading order may be used to represent a real system. Using this concept, the two-dimensional dynamics of the vortex system is reduced to determining the evolution of two point vortices of circulation Γ_1 and Γ_2, separated by a distance b. For the case of two counter-rotating vortices of equal magnitude (i.e. assuming $\Gamma_1 = -\Gamma_2$ and $|\Gamma_{1,2}| = \Gamma$, the two vortices induce a constant velocity along a straight line, perpendicular to the line connecting them, which is given by the equation:

$$U = \frac{\Gamma}{2\boldsymbol{p}b}. \qquad (6)$$

In the simulation, the self-advection speed of the vortex pair is subtracted such that the vortices remain in the computational domain.

Initial Conditions

Each vortex grows independently as a function of time due to viscous dissipation. Given an initially Gaussian cross section with radius a_0 the characteristic radius may be given as a function of time by:

$$a(t^*) = \sqrt{a_0^2 + 8\boldsymbol{p}\frac{t^*}{b^2}\text{Re}},$$
$$t^* = \frac{t}{t_c} = \frac{t\Gamma}{2\boldsymbol{p}b^2}. \qquad (7)$$

Here a_0 is the initial radius of the vortex, t^* is the normalised time unit, and t_c is the characteristic time for instability growth. In this study, a_0 was set to unity. The analytical study of Lacaze et $al.$ (2006) assumed no viscous dissipation, and hence no growth of the vortex radius over time. To accurately compare growth rates and mode structure with the analytical results of Lacaze et $al.$ (2006), it was essential that the vortex core did not grow appreciably within the linear growth region.

RESULTS

Two-Dimensional Initialization

The basic flow is obtained by a two-dimensional numerical simulation. The simulation is initialized with two counter-rotating Gaussian vortices without axial flow, each with an axial vorticity field provided by equation 1. This initial condition does not form a solution to the Euler (or Navier Stokes) equations. Thus, there is first a rapid "relaxation" phase during which the vortices equilibrate with each other. Then, the quasi-steady state which is obtained after the relaxation process is advected at a constant speed and slowly evolves due to viscous diffusion. The properties of the quasi-steady state have been analysed in Le Dizès and Verga (2002). The two-dimensional simulation is stopped once the relaxation process is complete. At this stage, both vortices are elliptic in cross section.

During the relaxation process, the mean vortex radius, $a,$ has slightly increased due to viscous diffusion and it is this new value which is considered for length scale normalisation. The 2D evolution of the axial flow is completely decoupled from the dynamics of the other velocity components and can be treated separately. It satisfies the same advection-diffusion equation as the axial vorticity. Thus, if we consider an axial flow velocity field proportional to the axial vorticity, we automatically form a solution. But, for such a solution, the axial flow is in the opposite direction when comparing either vortex with the other. Because, in most applications, vortices possess axial flow in the same direction, we have also integrated the advection-diffusion equation with an initial condition defined by

$$W(t=0) \propto \left|\boldsymbol{w}_z(t=0)\right|. \qquad (8)$$

Three dimensional Results

While several values of W_o were considered for this investigation, the findings for only two of them will be discussed here – this restriction has been made such that the modes with highest growth rate (and hence those of most interest) are reported here. The first simulation reported is the previously studied case of the Batchelor vortex pair in the absence of an axial velocity component (an Oseen vortex), the results of which allow comparison of the current numerical technique with several other investigations. The second case is for $W_0 = 0.482$, this allows direct comparison with the findings of Lacaze et $al.$ (2006). In each case the axial wave number was chosen such that the region of maximum growth rate was considered. Therefore, for the case where $W_0 = 0$, $k = 2.3$ and for $W_0 = 0.482$, $k = 1.9$ (see figure 3). In both cases $a_0 = 1$.

Figure 4 is an isosurface plot of the two vortices taken at several non-dimensional times, for the case of $W_0 = 0$ and $k = 2.3$. In the top left image, representing $t^* = 2$, the two vortices are parallel and appear to be straight, however close examination reveals that each vortex exhibits a small perturbation. At later times, a sinusoidal oscillation is observed in both vortices. This mode is a Kelvin mode of type (-1,1). The perturbation is of the same form as the small wavelength instability observed in previous

experiments (for an example see figure 2). Within an individual vortex, the instability forms in a direction 45^0 from the line directly linking the two vortices. This is in agreement with prior investigations, and with the analytical theory governing the growth of the instability.
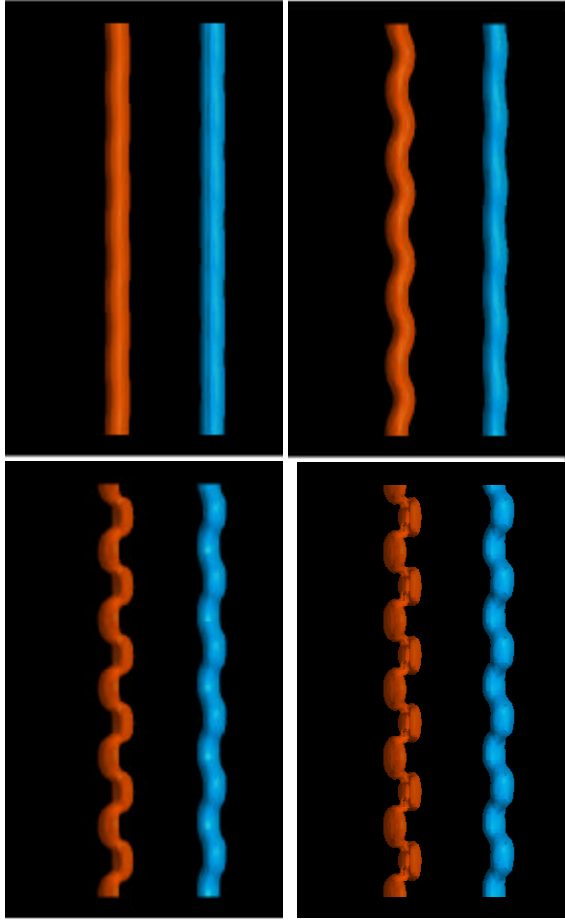
Figure 4: Isosurface images of the vortex pair at various instances of time, top-left $t* = 2$, top-right $t* = 4$, bottom-left $t* = 10$, bottom-right $t* = 12$; showing the growth of the mode (-1,1) instability. Here, $W_0 = 0$, and $k = 2.3$.
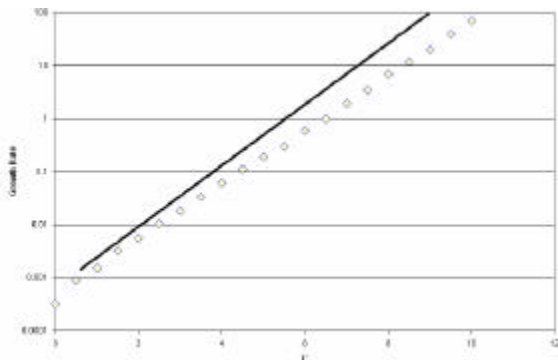
Figure 5: Growth rate, σ, as a function of normalized time, $t*$, for $W_0 = 0$ and $k = 2.3$; mode (-1,1). Solid line is from analytical estimates of previous studies, symbols are from the current study.

Figure 5 shows the growth rate of the instability as a function of $t*$. The solid line is the growth rate estimated analytically by Lacaze *et al.* (2006), the diamonds are measured growth rate values from the current numerical investigation. Overall, good agreement was found between the analytical investigations and the current numerical investigations. However, for high values of $t*$ ($t* > 5$), the numerical simulations indicate that the mode does not increase at the same rate as the analytical work does.

It is postulated here that the difference between the results rests in a limitation of the analytical approach employed by Lacaze *et al.* (2006). The analytical work assumes that the vortex core does not grow in size over time. While this assumption may be appropriate for high Reynolds numbers, in the current investigation the vortex cores were found to grow appreciably during the growth period of the instability. With reference to figure 3, we see that the growth rate is dependent on *ka*. At the start of the simulation, *ka* = 2.3, whereas at $t* = 10$, *ka* = 2.4. Thus, over time the system moves away from the region of highest instability – accounting for the decrease in growth rate away from that predicted by theory.
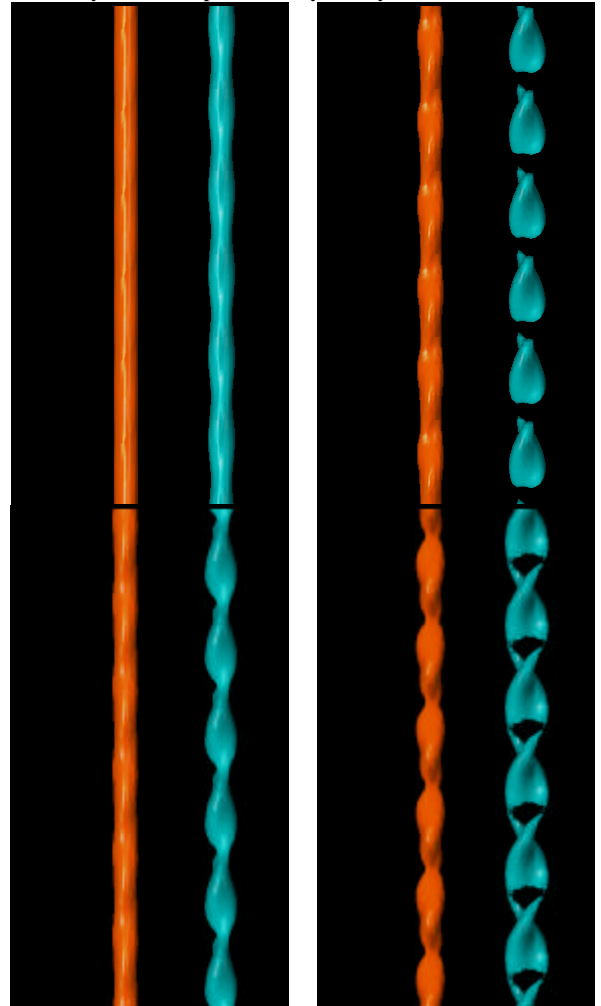
Figure 6: Isosurface images of the vortex pair at various instances of time, top-left $t* = 2$, top-rght $t* = 4$, bottom-left $t* = 10$, bottom-right $t* = 12$; showing the growth of the mode (-2,0) instability. Here, $W_0 = 0.482$, and $k = 1.9$.

Figure 6 is an isosurface plot of the two vortices taken at several non-dimensional times, for the case of $W_0 = 0.482$ and $k = 1.9$. As for the case depicted in figure 4, at low values of $t*$ ($t* = 2$), the two vortices remain parallel and relatively straight, however close examination reveals a small perturbation. At later times, an instability is observed in both vortices, whose spatial structure differs significantly when compared to mode (-1,1). This mode is a Kelvin mode of type (-2,0). As with the mode (-1,1), it is a coupling of two linear instability modes which are neutrally stable for an isolated vortex, but grow due to the influence of the second vortex. In this mode coupling the Kelvin mode 0 refers to a swelling and subsidence of the vortex core as a function of axis position. The top right image of figure 6 shows this mode component most clearly. The Kelvin mode -2 refers to the braiding of positive and negative perturbation vorticity components within each vortex core. In figure 6, this is most clearly observed in the bottom two images. Thus, the mode coupling (-2,0) shows both these features.

Figure 7 shows the growth rate of the perturbation as a function of normalized time. As with figure 5, the solid line is the growth rate estimated analytically by Lacaze *et al.* (2006), the diamonds are measured growth rate values from the current numerical investigation. Overall, good agreement was found between the analytical investigations and the current numerical investigations. However, as with the case of mode (-1,1) for high values of $t*$ ($t* > 5$), the numerical simulations indicate that the mode does not increase at the same rate as the analytical work does. Once again, with reference to figure 3, it is postulated that the growth in the vortex core size alters the preferred growth rate of the instability. For the present case, at the start of the simulation, $ka = 1.9$, whereas at $t* = 10$, $ka = 2.0$.
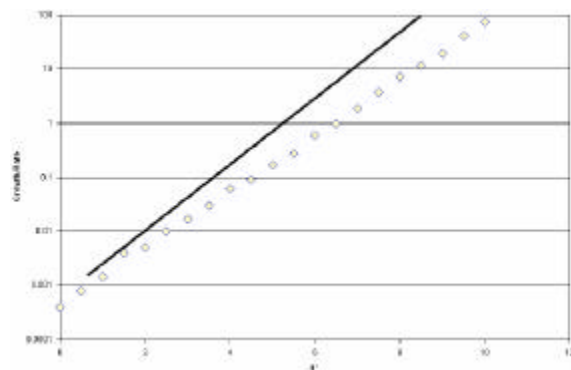
Figure 7: Growth rate, σ, as a function of normalized time, $t*$, for $W_0 = 0.482$ and $k = 1.9$; mode (-2,0). Solid line is from analytical estimates of previous studies, symbols are from the current study.

Comparing the two results, we see that the mode (-2,0) has a growth rate comparable to the mode (-1,1). This is of great interest when we consider that the mode (-1,1) has already been found to accentuate the Crow instability experimentally. It is hypothesized here that the mode (-2,0) could increase the growth rate of the Crow in a similar manner. Therefore, by ensuring that the axial velocity component is carefully chosen it may be possible to increase the growth rate of the Crow instability and hence decrease the spacing required between successive aircraft.

To confirm this hypothesis, further studies are necessary to compute the growth of the mode (-2,0) with an underlying Crow type instability, these investigations are continuing.

CONCLUSION

The current investigation has employed three-dimensional direct-numerical analysis to consider the linear growth of small wave (Kelvin type) instabilities which grow in the presence of a Batchelor vortex pair. The study has confirmed the recent analytical findings of Lacaze *et al.* (2006), for two cases in particular. The first case is for a flow with no axial velocity component, and the second is for a flow with an axial flow coefficient of $W_0 = 0.482$. In both cases, Kelvin-type instability modes were found with both exhibiting high growth rates. These modes may couple with existing large wavelength Crow instabilities to enhance vortex dissipation in the wake of aircraft.

REFERENCES

Arendt, S., Fritts, D. C., and Andreassen, O. (1997), "The initial value problem for Kelvin vortex waves", *Journal of Fluid Mechanics*, **344**, 181-212.

Ash, R. L. and Khorrami, M. R., (1995), "Vortex Stability", *Fluid Vortices*, (ed. S. I. Green), Chap. VIII 317-372, Kluwer Academic Publishers.

Batchelor, G.K. (1964), " Axial flow in trailing line vortices", *Journal of Fluid Mechanics*, **20**, 645-658.

Crow, S. C. (1970), "Stability theory for a pair of trailing vortices", *AIAA, J.*, **8**, 2172.

Fabre, D. and Jacquin, L., (2004), "Viscous instabilities in trailing vortices at large Swirl numbers", *Journal of Fluid Mechanics*, **500**, 239-262.

Fabre, D., Sipp, D., and Jacquin, L. (2006), "Kelvin waves and the singular modes of the Lamb-Oseen vortex", *Journal of Fluid Mechanics*, **551**, 235-274.

Karniadakis, G. E., Israeli, M., and Orszag, S. A. (1991), "High-order splitting methods for the incompressible Navier-Stokes equations", *Journal of computational Physics* **97**, 414-443.

Lacaze, L., Ryan, K., and Le Dizès S. (2006), "Elliptic instability in a strained Batchelor vortex", *Journal of Fluid Mechanics*, (in press).

Le Dizès, S. and Lacaze, L. (2005), "An asymptotic description of vortex Kelvin modes", *Journal of Fluid Mechanics*, **542**, 69-96.

Le Dizès, S. and Laporte, F., (2002), "Theoretical predictions for the elliptical instability in a two-vortex flow", *Journal of Fluid Mechanics*, **471**, 169-201.

Le Dizès, S. and Laporte, F., (2002), "Theoretical predictions for the elliptical instability in a two-vortex flow", *Journal of Fluid Mechanics*, **471**, 169-201.

Le Dizès, S. and Verga A., (2002), "Viscous interactions of two co-rotating vortices before merging", *Journal of Fluid Mechanics*, **467**, 389-410.

Leweke, T., and Williamson, C. H. K. (1998), "Co-operative elliptic instability of a vortex pair", *Journal of Fluid Mechanics*, **360**, 85-119.

Meunier, P. and Leweke, T. (2005), "Elliptic instability of a co-rotating vortex pair", *Journal of Fluid Mechanics*, **533**, 125-159.

Sipp, D. and Jacquin, L. "Widnall instabilities in vortex pairs", *Physics of Fluids*, **15**(7), 387-399.

Thompson, M. C., Hourigan, K., and Sheridan, J. (1996), "Three-dimensional instabilities ithe wake of a circular cylinder", *Exp. Therm. Fluid Sci.*, **12**, 190-196.